Thermal Analysis of a Gas Centrifuge

Andrade, D. A.; Bastos, J. L. F.; Maiorino, J. R.
Instituto de Pesquisas Energéticas e Nucleares - IPEN
Reactor Analysis Department

Abstract

The centrifuge separation efficiency is the result of the composition of the centrifuge field to the secondary flow in the axial direction near to the rotor wall. For a given machine, the centrifuge field can not be altered and the effort to augment the separation efficiency should be concentrated on the secondary flow. The secondary flow has a mechanical and a thermal component. The mechanical component is due to the deacceralation of the gas at the scoop region. The thermal component is due to the temperature differences at the rotor.

This paper presents a thermal model of a centrifuge in order to understand the main heat transfer mechanisms and to establish the boundary conditions for a fluid flow computer code.

The heat transfer analysis takes into account conduction at the structure parts of the rotor and shell, radiation with multi-reflections between the rotor and the shell, and convection to the ambient.

INDEX

INDEX OF FIGURES

INDEX OF TABLES

Introduction

The physics of the flow in the rotor is well described by several authors [1,2,3,4] showing that the separation efficiency of a centrifuge is a result of the composition of the centrifuge field to the secondary flow (countercurrent) in the axial direction near to the rotor wall (Figure 1). For a given machine, the centrifuge field can not be altered and the effort to improve the separation efficiency should be concentrated on the secondary flow. The secondary flow has a mechanical and a thermal component. The mechanical component is due to the deacceralation of the gas at the scoop region. The thermal component is due to the temperature differences at the rotor. There are four fundamental manners to generate or intensify the secondary flow in the rotor [5];

(a) Control of the temperature difference between the top and bottom caps (End Cap Thermal Drive);
(b) Control of the rotor axial temperature profile (Wall Thermal Drive);
(c) Optimization of the Scoop system (Scoop Type Drive);
(d) Feed project (Feed Drive).

The temperature difference between the end caps (a) and the axial temperature profile (b) are responsible for the convective countercurrent of the gas near to the rotor wall. The scoops together with the baffle generate a mechanical countercurrent.
The feed position is designed in such a way that it does not disturb, or disturb the least possible, the composed countercurrent mentioned above.

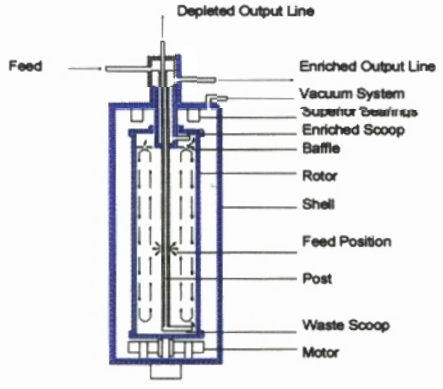

Figure 1 - Gas centrifuge sketch

For a given geometric configuration of the device, one can act only on the temperature field at the end caps and axial profile of the rotor in order to alter the secondary flow. Therefore, it is proposed in this paper a detailed study of the heat transfer phenomena for the centrifuge to have a better understanding of the temperature field and the main heat flux paths.

Due to the difficulties of instrumentation and high cost involved, a numerical approach for the problem, based on the Nodal Method, was adopted.

Thermal Model

The heat transfer mechanisms considered in this model are:

- Heat conduction at the several parts of the frame,
- Radiation for the regions under vacuum,
- Natural convection to the ambient.

The numerical model is based on the Nodal Method since it is suitable to deal with complex geometries and simultaneous heat transfer modes. The code used for the simulations is called "PCTER" and it was initially developed for thermal analysis of satellites [6]. PCTER has four main programs:

- GEOTRI which is a three dimensional pre-processor and is responsible for the calculations of the conduction and convection conductances;
- GEO that estimates the view factors;
- RAD that estimates the radiative conductances taking into account multi-reflections effects;
- ANATER which is the solver of the non-linear algebraic system of equations.

TECPLOT, a commercial code, is used for post-processing.

Due to the geometrical complexity of the centrifuge, some simplifications were necessary. Figure 2 is a schematic representation used to generate the thermal model. In this figure

the elements that compose the centrifuge are represented by blocks that will be divided into nodes later.

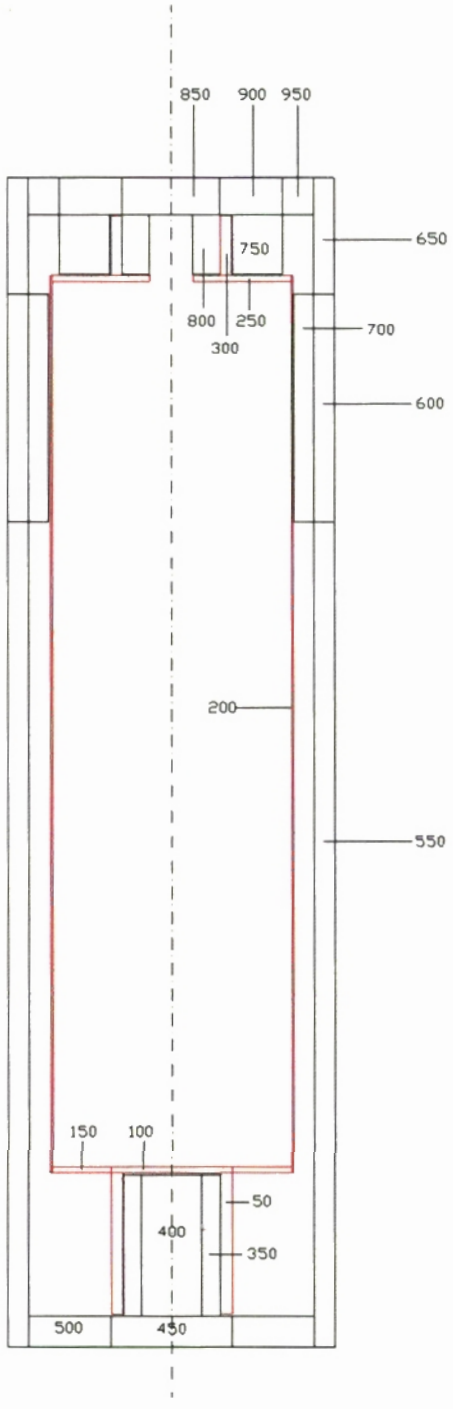

Figure 2 - Schematic centrifuge representation

Table 1 shows a list of the blocks for the model:

BLOCK	ELEMENT
50	Inferior rotor (motor)
100	Inferior end cap part- Internal cylinder
150	Inferior end cap part- Internal cylinder
200	Internal cylinder
250	Superior end cap part- Internal cylinder
300	Superior end cap part- Internal cylinder
350	Motor wiring
400	Motor core
450	Inferior end cap part- Shell
500	Inferior end cap part- Shell
550	Shell part
600	Shell part
650	Shell part
700	Molecular pump
750	Axial bearing
800	Superior bearing part
850	Superior end cap part- Shell
900	Superior end cap part- Shell
950	Superior end cap part- Shell

Table 1 - Description of each block of the model

A block can represent a simple element of the centrifuge. An example is block number 700 which represents the molecular pump. It can also represent a complex element like the motor for example (block number 400) which is composed by different materials. In this case, for the correct representation of the heat transfer phenomena, the equivalent thermal conductivities for each direction regarding all the different materials must be calculated. Material properties were taken from [7,8].

The calculation of the radiative changes needs the knowledge of the view factors for the surfaces. These view factors are calculated for plane geometries. Therefore, for the

calculation of these factors it was necessary to facet the cylindrical geometry of the centrifuge to obtain a regular polygon as shown in Figure 3. This figure presents a cross section of the cylinder and shell and the direct radiative changes between the surfaces. The multi-reflection effects connecting all nodes are not represented in order to have a clearer figure. After the calculation of the radiative conductances, regarding that the problem is axisymmetric, the eight surfaces which compose a specific region of the centrifuge are merged into a unique node. As a consequence, there are several radiative conductances between two nodes. The calculation method used by GEO depends on the existence or not of blockage between two surfaces. If there is no blockage, the view factors are calculated by the Boundary Integration Method which is fast and precise. If a blockage is present the code uses the Double Discretization Method which is slower and less precise. The effects of the multi-reflections between the surfaces are estimated by the Gebhart Method using the RAD routine.

Figure 4 shows the nodal division for the different elements of the centrifuge. In Figure 4(a) the motor (blocks 350 and 400) and the inferior shell end cap (blocks 450 and 500) are represented. Figure 4(b) shows an assembly of the motor (blocks 350 and 400), inferior shell end cap (blocks 450 and 500), motor rotor (block 50) and the inferior end cap of the cylinder (block 100 and 150). Figure 4(c) represents the same blocks of Figure 4(b) added to the cylinder (block 200) and the superior end cap of the cylinder (blocks 250 and 300). Note that the side wall of the cylinder was divided into fourteen nodes in the axial direction in order to have a precise temperature gradient indication. Figure 4(d) is Figure 4(c) plus the superior end cap of the shell (block 850, 900 and 950). Finally, the complete model is represented in Figure 4(e). A wire frame representation of the shell (blocks 450, 500, 550, 600, 650, 850, 900 and 950), molecular pump (block 700) and axial bearing (block 750) is shown.

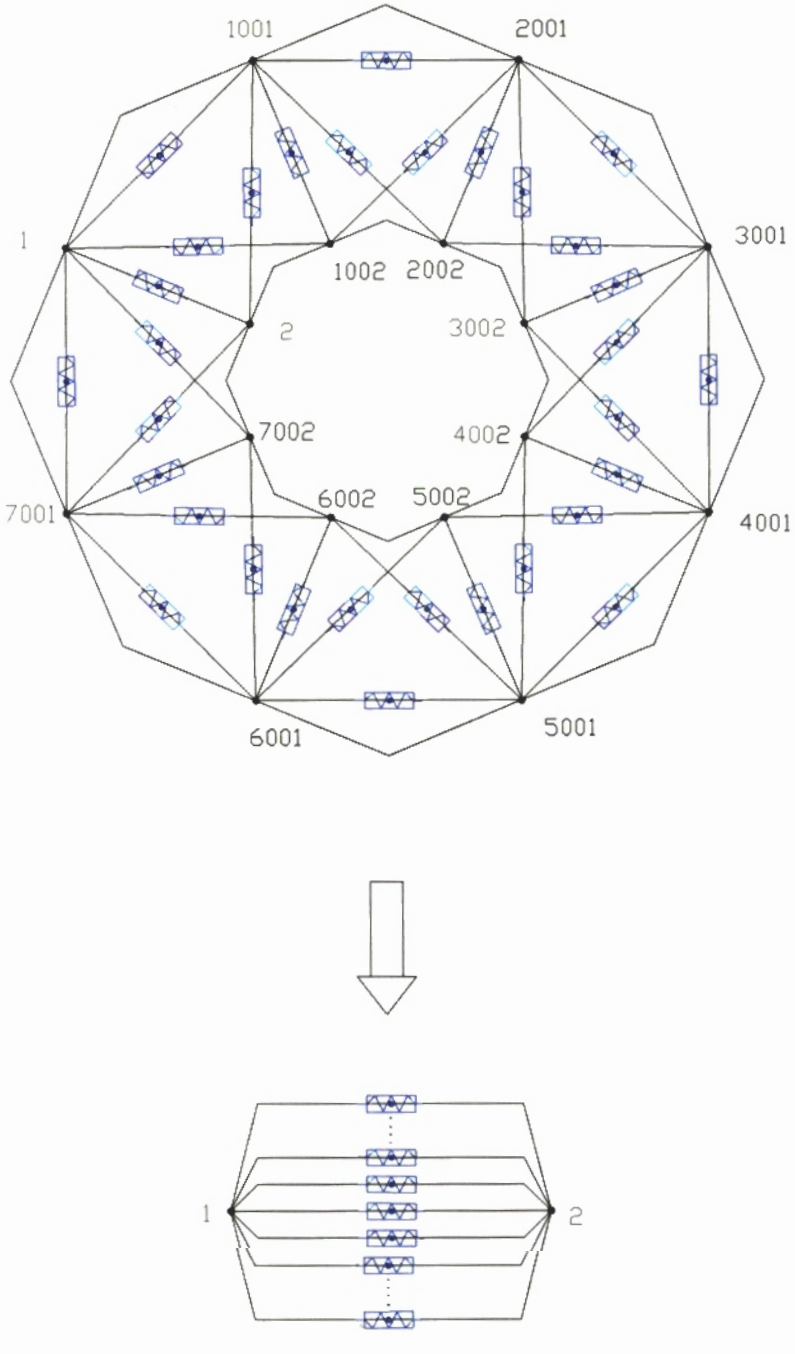

Figure 3 - Representation of a cross section of the cylinder and shell

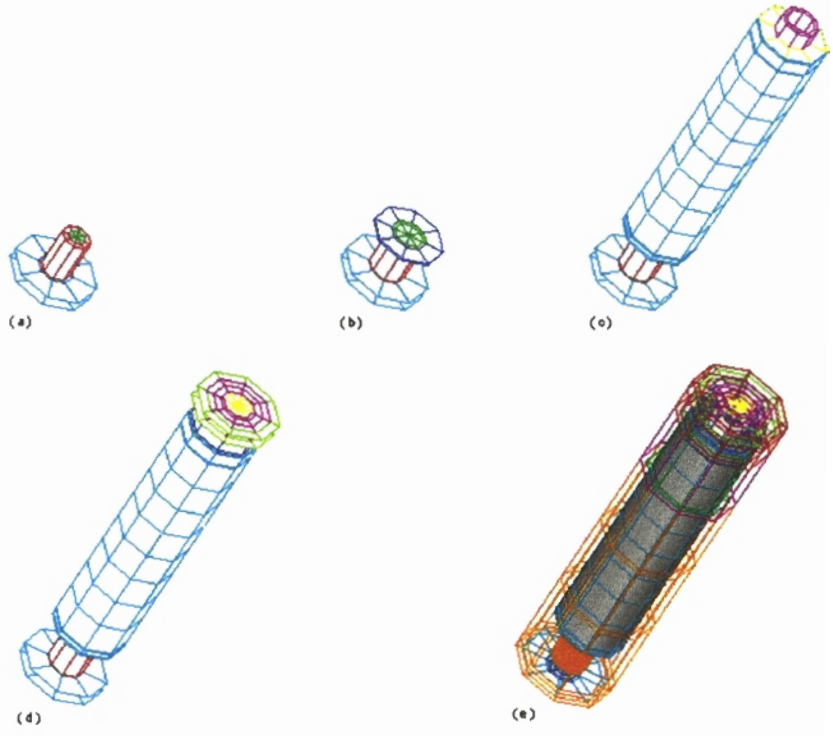

Figure 4(a,b,c,d,e) - Nodal division of the different elements of the centrifuge

The calculation of the convective and conductive conductances for the three directions is done by the routine GEOTRI. This code permits cylindrical and rectangular geometry calculations. For the conduction conductances it is necessary to know the conductivity of

the materials of each block. Table 2 shows the thermal and optical properties used. Thermal conductivities of the different blocks represent the conductivity of a unique material for simple blocks and an equivalent value which regards the different material volumes for a complex block.

Block	$K_{equivalent}$ (W/mK)		$\varepsilon = \alpha$
	k_r	k_z	
50	76.11	26.42	0.13
100	20.10	20.10	-
150	20.10	20.10	0.13
200	20.10	20.10	0.60
250	20.10	20.10	-
300	68.72	26.70	-
350	9.34	35.78	-
400	15.00	15.00	-
450	45.00	45.00	-
500	45.00	45.00	0.08
550	45.00	45.00	0.08
600	45.00	45.00	-
650	45.00	45.00	0.08
700	234.0	234.0	0.50
750	10.82	43.89	0.20
800	10.13	5.58	-
850	45.00	45.00	-
900	45.00	45.00	-
950	45.00	45.00	0.08

Table 2 - Thermal and Optical properties for the model

The main sources of heat in this centrifuge model are: motor, molecular pump, axial bearing and the flowing gas in contact with the scoops. The estimate of the heat fluxes generated for each part is very much complex. The values in Table 3 are based on theoretical results. Note that the heat flux generated by the waste scoop is 4 W and the product scoop is 2 W. These heat fluxes are due to the friction between the flowing gas and the scoops. The heat flux generated at the waste scoop is higher due to its position in a higher pressure region of the gas flow.

Block/Node	Heat fluxes (Watts)
200/202	4
200/211	2
350/350	15
400/400	5
700/700	5
750/750	5

Table 3 - Heat Fluxes

No heat exchange is considered between the flowing gas and the internal wall of the rotor. This approximation is not realistic, but it seems that the coupling between the structure and the gas flow is more important for the thermal component of the secondary flow of the gas than for the thermal behavior of the centrifuge structure. Natural convection is considered between the shell and the ambient temperature. A simple heat transfer was considered based on classical correlations of the literature.

Results

Figure 5(a) shows the temperature distribution for the cylinder. Figure 5(b,c) show the temperatures of the shell. The central region of the inferior shell end cap presents the highest shell temperature due to its position near to motor. The side wall of the shell presents temperatures near to the ambient.

The maximum temperature for the cylinder occurs at the region of the waste scoop and motor which are subjected to the highest heat fluxes. The maximum temperature at this region is $T = 59.30\,^{\circ}C$.

The temperature of the inferior end cap is higher than the superior, $\Delta T = 24.50^{\circ}C$, therefore there is a strong convective countercurrent.

The axial temperature distribution of the rotor wall varies from $T = 57.50\,^{\circ}C$, inferior end cap, $T = 59.30\,^{\circ}C$, waste scoop, $T = 27.30\,^{\circ}C$ near the pump region and $T = 33.00\,^{\circ}C$ for the superior end cap. Therefore the maximum temperature difference at the cylinder is $\Delta T = 32.00^{\circ}C$.

Sensitivity analysis to the scoop position

Figure 6 shows the thermal behavior of the centrifuge changing the scoops position. The waste scoop is now positioned at the superior part and the product scoop is located at the inferior part of the rotor.

The maximum temperature for the rotor is smaller for this case and occurred at a different region. Due to the good radiative coupling between the molecular pump and shell, the heat flux generated at the waste scoop is easier evacuated. The maximum and minimum values for the cylinder are $T = 45.40^{\circ}C$ and $T = 27.90^{\circ}C$ respectively. In this case the maximum temperature difference is $\Delta T = 17.50^{\circ}C$.

The end caps temperatures are very close. Superior end cap $T = 42.93^{\circ}C$, inferior end cap $T = 41.20^{\circ}C$. The end caps temperature difference is $\Delta T = 1.73^{\circ}C$. The axial distribution in the rotor is nearly symmetric.

Sensitivity analysis to the optical material properties

Since most of the heat fluxes generated by the motor and the scoops are evacuated by radiation between the cylinder and shell, this model considers the effect of the emissivities on the thermal behavior of the centrifuge. The emissivities considered are those of the material submitted to different treatments.

The emissivities of blocks 50,150 correspond to the steel superficially treated with zinc and chromium. Blocks 200, 500, 550, 650 and 950 correspond to oxidized steel and block 700 to anodized aluminum. The emissivity of block 750 is kept the same (Table 4).

Figure 7 shows the temperature distribution for the rotor. The average temperature of the centrifuge is smaller than the first configuration. The maximum and minimum values for the cylinder are $T = 41.97^{\circ}C$ and $T = 21.95^{\circ}C$ respectively. The temperature difference between the end caps is $\Delta T = 6.97^{\circ}C$.

Block	Emissivities
50	0.30
150	0.30
200	0.50
500	0.50
550	0.50
650	0.50
700	0.50
750	0.20
950	0.50

Table 4 - Material emissivities- Sensitivity analysis

Conclusions

The thermal behavior of a countercurrent centrifuge was analyzed by the Nodal Method taking into account the main heat transfer mechanisms involved. The heat fluxes generated at the motor and scoops are mainly evacuated by radiation between the cylinder and shell.

Sensitivity analyses were performed showing that the temperatures distribution of the centrifuge are strongly modified inverting the scoops position. Positioning the waste scoop at the superior region of the cylinder the maximum temperature is $13.90^{\circ}C$ lower compared to a configuration where this scoop is at the inferior position.

The optical properties of the materials showed to be another important point. Since the radiative exchange is the main mechanism to evacuate the heat fluxes, a better coupling between cylinder and shell reduces significantly the average temperature of the centrifuge.

This study helped to determine some important parameters for the temperature distribution at the rotor and end caps, however only a complete analysis coupled to the flow model will permit the evaluation of the best configuration for the separative efficiency.

Future Development

An interface to couple this thermal model with the hydrodynamic model (Maliska,C.R.; Silva, A.F.; Andrade, D.A. [9]) will be developed. This interface is under development, since the meshes and nature of these models are strongly different. The results of the complete model, Thermal coupled to the Flow model, will be presented soon.

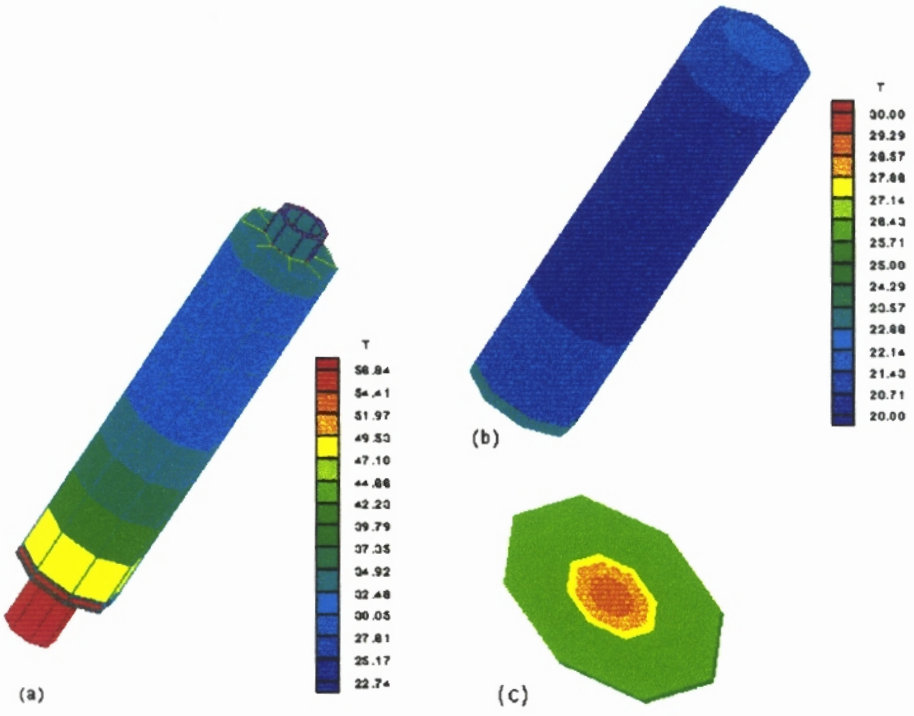

Figure 5(a,b,c) - Temperature distribution for the rotor, Shell and Shell detail

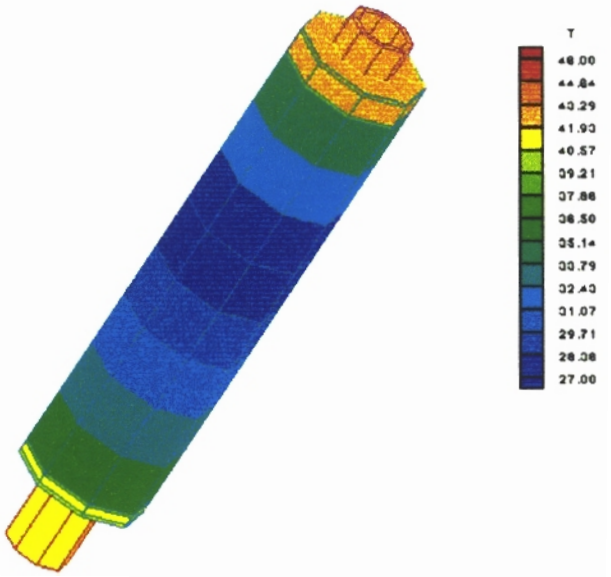

Figure 6 - Temperature distribution - Sensitivity to the scoops position

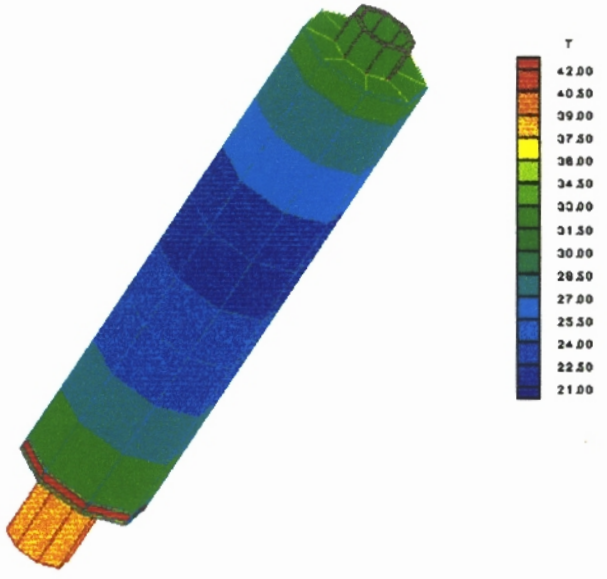

Figure 7 - Temperature distribution - Sensitivity to the optical material properties

Bibliography

[1] Greespan, H. P., **"*Theory of Rotating Fluids*", Cambridge University Press,** London (1969).

[2] Sakurai, T. and Matsuda, T., "*Gasdynamics of a Centrifugal Machine*", **Journal of Fluid Mechanics.** Vol. 62(4), 727-737 (1974).

[3] Stewartson, K., "*On Almost Rigid Rotation*", **Journal of Fluid Mechanics.** Vol. 3, 17-26 (1957)

[4] Bark, F. and Bark, T. H., "*On vertical boundary Layers in a Rapidly Rotating Gas*", **Journal of Fluid Mechanics.** Vol. 78(4), 749-762 (1976).

[5] Soubbaramayer - "*Centrifugation*" - **In: Villani, S.; ed. Uranium Enrichment**, Springer Verlag, Berlin, 1979;

[6] Bastos, J.L.F.; Muraoka, I. ; Cardorso, H. P. - "*Pacote de Análise Térmica - PCTER*" - **Anais do 1º Simpósio Brasileiro de Tecnologia Aeroespacial** - august - 1990 - São José dos Campos - SP - Brazil.

[7] Siegel, R. ; Howell, J.R., "*Thermal Radiation Heat Transfer*", **McGraw-Hill**, 1972.

[8] Özisik, M.N., "*Heat Transfer - A Basic Approach*", **McGraw-Hill**, 1985.

[9] Maliska, C.R.; Silva, A.F.; Andrade, D.A. - "*A Strong Coupling Procedure for the Segregated Solution of Rotating Flows*" - **Proceedings of the Third Workshop on Separation Phenomena in Liquids and Gases** - August - 1992 - pag 223-232 -Charllottesville - Virginia - USA.